Structural Analysis of Historical Constructions, New Delhi 2006
P.B. Lourenço, P. Roca, C. Modena, S. Agrawal (Eds.)

A Theoretical and Experimental Stress Distribution in Reinforced No-Tension Walls

A. Baratta
University of Naples "Federico II", Department of Structural Engineering, Naples, Italy.

I. Corbi
University of Naples "Federico II", Department of Structural Engineering, Naples, Italy.

ABSTRACT: In this paper a computational procedure for two-dimensional equilibrium problems, which are representative of the behaviour of masonry walls loaded by in-plane forces, is analyzed. The solution is searched through an optimisation procedure according to the *conjugate gradient method* interpolated with *relaxation intermediate steps.* The procedure is tested from a computational point of view, with reference to a masonry wall with a central opening subject to a varying horizontal force. Moreover some laboratory tests concerning a masonry panel designed to be similar as the theoretical model are reported, and the comparison with the results relevant to some FRP reinforcements applied on the panel after the collapse are discussed.

1 INTRODUCTION

New perspectives in approaching preservation and consolidation issues related to historical masonry constructions are coming, in the recent years, by the contribution of many different disciplines, inspiring a number of more and more sophisticated refurbishment techniques and adaptation interventions. Nowadays some valid alternatives to ordinary refurbishment techniques are offered by the factory with the development of new materials originally intended for the application in different fields than the construction sector, i.e. the Fibre Reinforced Polymers (FRP), a new class of composite materials born many tens of years ago for military and aerospace use.

An increasing interest about the composites from the factory and research fields has established their use both into pre-damage and post-damage strategies, particularly for ancient constructions since they are able to provide effective and low invasive reinforcement interventions (Briccoli Bati and Rovero 2000). Under such a perspective, the exploitation of the composites seems particularly suitable for applications related to the restoration and/or reinforcement of ancient constructions (Schwegler 1994, Traintafillou 1996, El-Badry 1996, Briccoli Bati and Rovero 2000), on the other hand, the adoption of innovation materials and technologies, including smart materials, is strongly time limited since a very deep knowledge of their behaviour and interaction with the structure is required in order to avoid risks of loss or irreversible damage of the heritage.

2 FIBRE REINFORCED POLYMERS

Fibre Reinforced Polymers (FRPs) are basically composites characterized by a polymeric matrix reinforced with continuous fibres (Schwegler 1994, Traintafillou 1996), which exhibit desirable features, such as high mechanical properties, lightweight, high resistance to chemical agents and corrosion, increased fatigue resistance, reliability and durability, low thickness, adaptability and easy applicability to complex structural shapes, low invasiveness and reversibility.

Composites are materials produced by the combination of two or more distinct physical phases: a discontinuous phase, which is called *fibre*, and a continuous one, which is called *matrix*, where the fibres are dispersed inside. In the construction industry, the term is generally utilized for polymers reinforced with high strength high modulus continuous laid up in layers to form an engineered material. A wide range of amorphous and crystalline materials can be used as the fibre in FRP materials. In the construction industry the most common fibre used are: glass fibre (type E-glass, A-glass, AR-glass, S + R glass and high strength glass), carbon fibre (type I, II and III) or aramid fibre (see Table 1 for a comparison between the principal mechanical characteristics of FRP fibres).

Table 1 : Typical values of some mechanical characteristics of FRP fibres.

Fibre	Density	Elastic Modulus	Tensile Strenght	Ultimate Elongation
	kg / cm^3	GPa	MPa	%
Carbon Fibre	1.7 ÷ 1.9	200 ÷ 600	2000 ÷ 3000	1
Glass Fibre	2.5	70 ÷ 85	3000 ÷ 4500	4 ÷ 5
Aramid Fibre	1.45	60 ÷ 130	2700 ÷ 3000	2 ÷ 10
Steel	7.8	200 ÷ 210	500 ÷ 2000	2 ÷ 10
Aluminium	2.8	75	500	10
Titanium	4.5	110	1200	14

Carbon fibre can be used separately or in conjunction with the glass fibre as a hybrid to increase the stiffness of a structural member or the area within a structure, so that the stiffness exceeds the value possible using only glass fibre. Moreover, in order to increase stiffness to the composite instead of glass fibres can be used aramid fibre. The fibres are produced as bundle of filaments, called strand, which are usually combined to form thicker parallel bundles, called *roving*. Roving can be manufactured by a direct technique (*direct roving*) in which all the filaments needed in the final roving (up to 4800) are all drawn simultaneously from one bushing and are used in weaving, pultrusion and filament winding. Strand may also be twisted to form several types of yarn; roving or yarn may be used either individually or in the form of a woven fabric. The embedded fibre matrix is responsible not only for keeping the fibres together but also to protect them against environmental and localised effects. The resin of the matrix can be polyester, urethane, vinilester or epoxy; in most cases epoxy resin is used. Fibres are embedded in resin before application in case of pultruded strips and during application in case of fabrics. The resin plays the double role of embedding and gluing of fabrics. In case of strips, embedding is ensured during pultruding while gluing is carried out by a separate resin (which is also generally epoxy based). The main characteristics of resins are: modulus of elasticity failure strain, shrinkage, glass transition point, coefficient of thermal expansion. The hardening rate of resins depends on their temperature; the higher the temperature the higher the hardening rate is. Two main types of polymer are usually used for resins: thermo-sets and thermo-plastics. The thermo-setting polymers used in the construction industry are the polyesters and the epoxides; the thermoplastic resins used in composite manufacture are: poly-olefins, polyamides, vinyl polymers, poly-acetates, poly-sulphones, polycarbonates, polyphenylenes and poly-imides.

For structural applications it is mandatory to achieve some degree of flame retarder. Fire retardants are usually incorporated in the resin itself or as an applied gel-coat. Fillers and pigments are also used in resins for a variety of purposes, the former principally to improve mechanical properties and the latter for appearance and protective action. The exploitation of the FRP material's properties in the field of structural rehabilitation, is acquiring an increasing interest by the international scientific community, due to the circumstance that they may respond in a satisfactory way to needs rarely met by the adoption of traditional materials and methodologies. In details, because of their high strength in tension and low flexural rigidity, Fibre Reinforced Polymers, are viable candidates for increasing the mechanical resistance of those structures made by materials that exhibit a very low tensile resistance, such as masonry, and that obviously represent the big part of the ancient or simply old constructions of many historical regions. Moreover, FRPs couple low weight, good resistance to chemical attacks, low electrical conductivity, low invasiveness and reversibility to their high stiffness and strength, which are all very desirable features especially when referring to monumental and historical constructions; in

details the easy applicability, the marginal invasiveness and the absolute reversibility of FRP provisions allow to account both for the structural safety, also with reference to the seismic risk, and for the respect of the original structural apparatus of the ancient constructions.

Actually of basic importance for the effectiveness of the provision is the right orientation of the fibres, which should optimally exploit the high fibres' anisotropy in order to compensate the low tensile resistance of structural masonry elements.

3 NON-RESISTING TENSION MODEL

The feature that mainly characterizes the behaviour of masonry is its very low tensile resistance, which pushes toward the adoption of Non-Resisting Tension (NRT) models. The basic NRT model exhibits a simple linear elastic behaviour under compression stress states and no resistance in tension, thus resulting in an overall fragile non-linear behaviour. It has been shown (Heyman 1969) that the loading capacity of NRT structures can be investigated by means of the tools of the Limit Analysis (L.A.) theory. On the other hand, the study of the intermediate crack situation can not be performed by L.A.-techniques, while the elastic analysis of the masonry tissue under the assumptions of perfect integrity of the structure can lead to poorly significant results. Optimisation (stress or strain) procedures (Rao 1978), deriving from the implementation of the basic variational methods extended to NRT models (Baratta and Toscano 1982, Baratta and Voiello 1988, Baratta 1991, Baratta and Corbi 2005), can then, be developed. Since the inner constraint is mainly concerned with the stress or the fracture strain components (according to the used method), a discretization with constant stress/constant strain elements is adopted.

3.1 Computational procedure

A computational procedure for analysing the behaviour of NRT masonry walls loaded by in-plane forces has been developed, which searches for the solution by means of the Total Potential Energy (TPE) approach.

First of all, some kinematic variables, i.e. the fracture strain $\boldsymbol{\varepsilon}_f$ and the nodal displacement $\mathbf{u}$ vectors, must be assumed, and a constraint on the fracture strain tensor $\boldsymbol{\varepsilon}_f^e$ in the generic *e*-th element, which is required to be positive semi-definite, must be imposed.

The search of the constrained minimum of the energy functional is performed by iterating two steps: **step 1** constrained minimization ($\boldsymbol{\varepsilon}_f^e \geq \mathbf{0}$) of the energetic functional $\mathcal{E}$ by varying the fracture strain components under fixed displacements; **step 2** absolute minimization of the energetic functional $\mathcal{E}$ by varying the displacement components under fixed fracture strain. The **step 1** is performed by relaxing the tensile stresses (i.e. $\boldsymbol{\sigma}^e \leq \mathbf{0}$) within each element usually resulting in the violation of equilibrium with applied loads, while the **step 2** restores the overall equilibrium. The procedure starts from a reference solution which coincides with the linear elastic one ($\boldsymbol{\varepsilon}_f^e = \mathbf{0}$). For a more detailed description of the iterative procedure see Baratta and Corbi (2004) In the following a synthesis of the two steps of the procedure is illustrated.

Step 1: the Total Energy is equal to the sum of the energies in the single elements plus the Potential Energy of the active loads. The energy in the *e*-th element depends only on the tensor $\boldsymbol{\varepsilon}_f^e$ and on the nodal displacements. The minimization of the total energy $\mathcal{E}$ just requires the minimization of the energy $\mathcal{E}_T^e$ in any single element. When considering the *e*-th deformations $\left(\boldsymbol{\varepsilon}^e\right)^T = \left(\varepsilon_x^e \;\; \varepsilon_y^e \;\; \gamma_{xy}^e\right) = \left(\mathbf{B}^e \mathbf{u}^e\right)^T$, with $\mathbf{B}^e$ the compatibility matrix of the element and $\left(\mathbf{u}^e\right)^T = \left(\mathbf{u}_i^T \;\; \mathbf{u}_j^T \;\; \mathbf{u}_k^T\right)$ the transpose of the displacement vector $\mathbf{u}^e$ collecting the displacements of the i,j,k nodes of the *e*-th element, the problem reduces to the following constrained minimization

$$\begin{aligned} &\text{Find} \quad \min_{\boldsymbol{\varepsilon}_f^e} \left[\mathcal{E}^e\left(\mathbf{u}, \boldsymbol{\varepsilon}_f^e\right)\right] = \min_{\boldsymbol{\varepsilon}_f^e} \left\{\frac{1}{2}\left[\left(\boldsymbol{\varepsilon}^e - \boldsymbol{\varepsilon}_f^e\right) \cdot \mathbf{C}^e \left(\boldsymbol{\varepsilon}^e - \boldsymbol{\varepsilon}_f^e\right)\right]\right\} \\ &\text{Sub} \quad \left\{J_{1f}^e \geq 0, \quad J_{2f}^e \geq 0\right. \end{aligned} \tag{1}$$

with J_{1f}^e, J_{2f}^e the first and second invariant of the fracture strain tensor.

Within each element, the solution is searched for, by looking for $\boldsymbol{\varepsilon}_f^e$ such that the relevant stress $\boldsymbol{\sigma}^e = \mathbf{C}^e\left(\boldsymbol{\varepsilon}^e - \boldsymbol{\varepsilon}_f^e\right)$ is purely compressive and co-axial with $\boldsymbol{\varepsilon}_f^e$. To this purpose one calculates

the purely elastic stress state in the element $\bar{\boldsymbol{\sigma}}^e = \mathbf{C}^e \boldsymbol{\varepsilon}^e$ and its principal components $\bar{\sigma}_1^e, \bar{\sigma}_2^e$; if $\bar{\sigma}_1^e \le \mathbf{0}, \bar{\sigma}_2^e \le \mathbf{0}$, then $\boldsymbol{\varepsilon}_f^e = \mathbf{0}$, i.e. the stress state is compatible and there is no need to add fracture; otherwise, it can be shown (see Baratta 1991) that the condition $\boldsymbol{\sigma} \cdot \boldsymbol{\varepsilon}_f = 0$ is verified in every element.

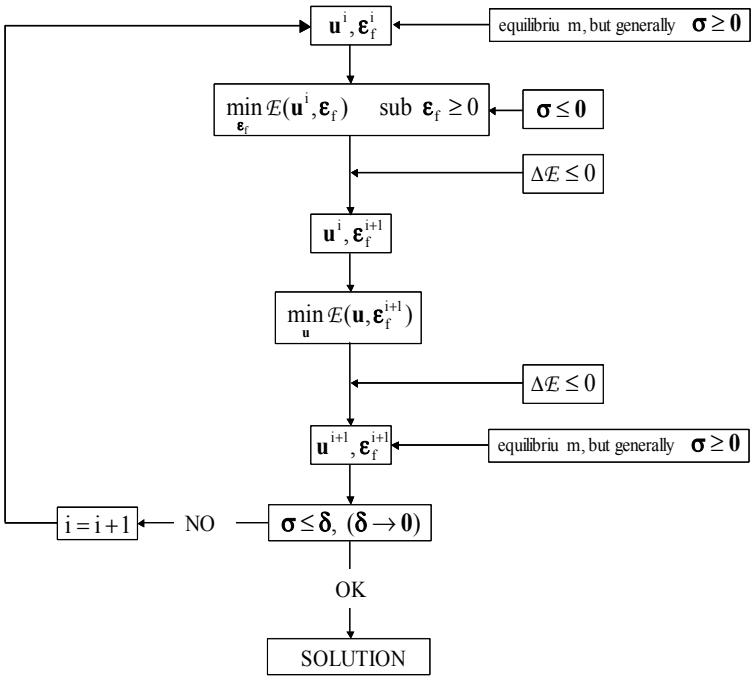

Figure 1 : Flow graph of the iterative procedure adopted in the numerical implementation.

Step 2: the nodal displacement vector **u** is no more equilibrated since the variation of $\boldsymbol{\varepsilon}_f$ at **step 1** has perturbed the equilibrium. In order to re-equilibrate the system, **u** is re-tuned in such a way that, by coupling **u** with the modified $\boldsymbol{\varepsilon}_f$, one gets an equilibrated solution, through an absolute minimization, which is performed by means of the method of the conjugate gradients (see Rao 1978) with constant $\boldsymbol{\varepsilon}_f$

$$\text{Find} \quad \min_{\mathbf{u}} \left[\mathcal{E}(\mathbf{u}, \boldsymbol{\varepsilon}_f)\right] = \min_{\mathbf{u}} \left[\mathcal{E}(\mathbf{u}, \boldsymbol{\varepsilon}_f)\right] \tag{2}$$

The flow graph reported in Fig. 1 shows the entire implementation of the procedure.

4 THEORETICAL STRESS DISTRIBUTION IN A MASONRY PANEL WITH A CENTRAL OPENING

The TPE (Total Potential Energy) approach above illustrated is applied to a masonry panel. The panel, which is characterized by geometric dimensions of 2.30 x 2.23 m, is realized with horizontal rows of square bricks, having staggered horizontal and vertical joints and with a central hole. The central opening in the wall is assumed to be reinforced by an architrave, which is included in the model as extensional and flexural elastic beams united to masonry.

In the procedure the masonry panel is assumed to be subject to vertical self-weight forces and varying horizontal force. The range of variation of the static force applied on the upper part of the panel's left side is assumed between 0.0 and 5000 N.

After selecting an appropriately dimensioned triangular mesh which covers all the wall having more elements where the stress distribution becomes much more important (Fig. 2a) the first operation consists of searching for the elastic solution on the displacements u_e. In particular, the calculus model refers to the discretization in 1536 constant stress/constant strain elements, jointed to each other by 825 nodes.

Starting from two considerations: i) relative tensile stresses $\boldsymbol{\sigma}^+$ are inadmissible if the solution on the displacements is imposed as equilibrated and congruent; ii) all the elements are assumed

with constant stress, so elastic strains $\boldsymbol{\varepsilon}_e$ and fracture strain $\boldsymbol{\varepsilon}_f$ are constant too; the iterative procedure consists of locking the displacements with null tension stresses, while the fracture strain field varies, then, after fixing the fracture strain field the displacements vary and thereafter the tension stresses are not zero. The final solution of the problem is found by means of subsequent iterations of the two steps as explained into the scheme of Fig. 1.

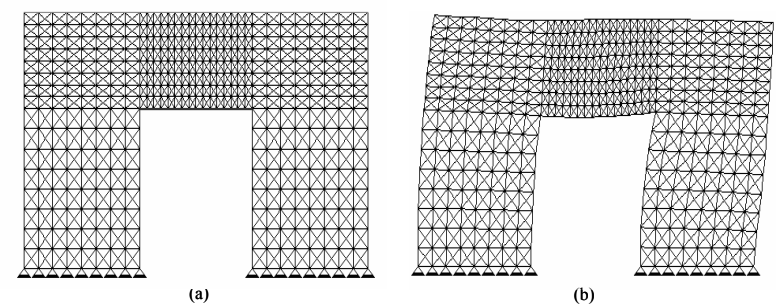

Figure 2 : (a) Finite element model of a masonry panel with holes, and (b) deformed configuration.

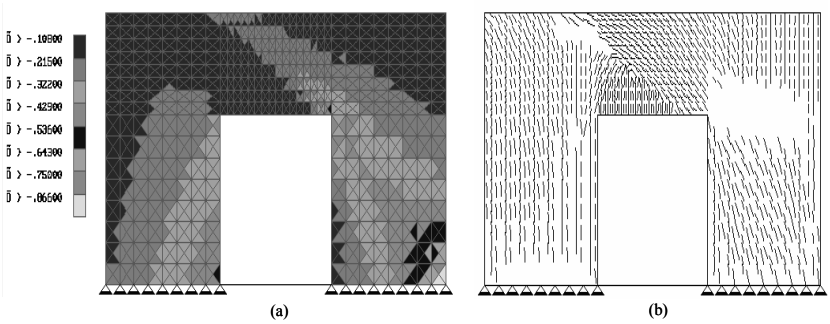

Figure 3 : (a) Compressive stress distribution, and (b) fracture distribution and orientation.

In Fig. 2a) the finite element model of the masonry wall considered for the numerical investigation is shown. The deformed configuration of the panel relevant to a force of 1000 N is depicted in Fig. 2b), where an amplification factor of 1000 has been adopted in order to emphasize the induced displacements. The compressive stress distribution in the panel and the fracture diffusion and orientation is plotted in Figs. 3a and 3b respectively.

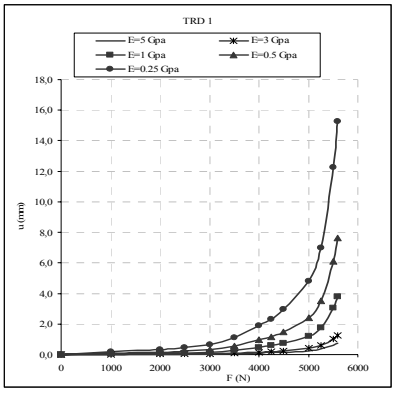

Figure 4 : Theoretical curves for different Young modulus.

Moreover, the procedure produces the theoretical curves of the displacements versus the force F at the location of the transducer 1 (TRD1) for different values of the Young modulus E, as shown in Fig. 4.

5 EXPERIMENTAL STRESS DISTRIBUTION

5.1 Experimental tests: a masonry panel with a central opening

In the following, the results obtained by means of some experimental tests developed on prototypes of masonry walls at the Laboratory of Materials and Structural Testing of the University of Naples "Federico II" are shown.

More specifically, a symmetrical masonry wall has been built with geometric dimensions as given in Fig. 5a. The panel is made of tufa bricks (type "yellow tufa of Naples", Italy) jointed by a pozzuolana mortar in order to confer a light additional resistance to the masonry. The masonry itself is characterized by unit weight γ=10300N/m^3 and Young modulus E=5.5 GPa. The wall has a central hole covered by a steel architrave, and a concrete fascia lightly reinforced by steel bars, in the upper part. A varying force has been applied in the middle left part of the panel, rather than on the top, in way to mitigate the proneness of the panel to sliding of bricks with respect to each other. The induced displacements at some selected points (1, 2 and 3 in Fig. 5a) of the panel are recorded by a monitoring equipment consisting of: i) 4 transducers, placed at different locations of the panel in order to record the absolute displacements, and ii) 15 strain-gauges, arranged in 3 blocks of 5 strain-gauges, each block is devoted to record the related strain situation. In details two transducers are located horizontally at two different heights on the panel left side (transducer 1 and transducer 2), and two in correspondence of the opening, one in horizontal position at the top of the right side of the hole (transducer 3) and the other one under the architrave at its middle point, which is devoted exclusively to control the panel deflection. In the first stage of the experimental tests some loading/unloading cycles are considered with the applied load consisting of a lumped increasing force in the loading phase; thereafter the unloading process is started. At every cycle the loading phase is stopped as the wall is approaching the collapse, i.e. as it enters the asymptotic phase of the force-displacement diagram, which is characterized by a strong increasing of the bending of the panel in its plane, by the degradation of the mortar in the bricks' joints and by the consequent loosing of bond between the tufa bricks (Fig. 6).

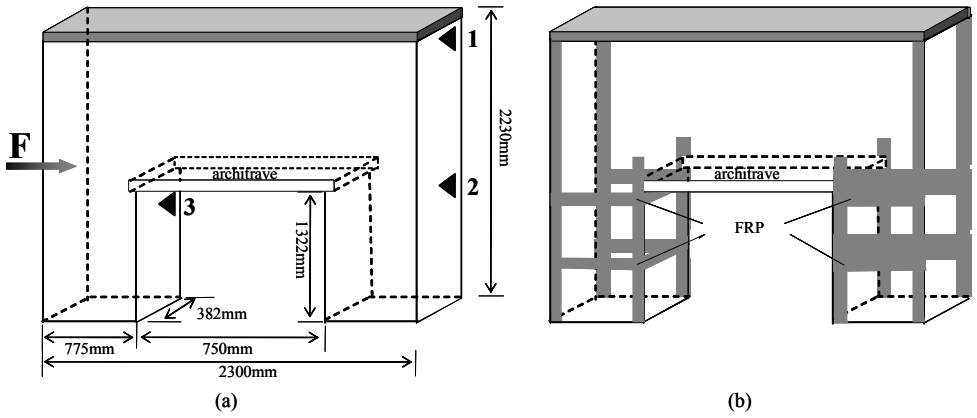

Figure 5: (a) Geometric dimensions of the tested masonry panel and (b) C-FRP reinforced masonry panel.

5.2 Experimental tests: reinforced masonry panel

In the following, the problem of reinforcing a masonry tissue is approached experimentally, in order to validate the FRP repair technique. So a reinforcement of the panel is realized by means of some continuous mono-directional FRP strips (Fig. 5b). The chosen reinforcement is designed taking into account the expected distribution of the tensile stresses in the wall, in that it is intended to test the theoretical analysis, rather than the effectiveness of the intervention.

The adopted reinforcement, produced by FTS, is a Betontex system GV330 U-HT, made of 12K carbon fibre, jointed by an ultra light net of thermo-welded glass. The mechanical characteristics of the employed carbon fibres are: tensile limit stress σ_{frp}= 4.9x10^8 kg/m^2, elastic modulus in traction E_{frp}=244x10^8 kg/m^2, limit elongation ε_{frp}=2%. The C-FRP strip is characterized by

thickness of 0.177 mm and depth of 200 mm. After roughly preparing the masonry support in order to render the application surface smoother, the FRP reinforcement is directly laminated on the masonry, at the same time with the impregnation of the fibres by means of a special bi-component epoxy resin. The application of the reinforcement is made after the masonry panel has been brought near the collapse threshold; then other loading/unloading cycles are developed on the wall with the loading equipment and the monitoring equipment placed in the same configuration as for the non-reinforced panel (Fig. 5b). Moreover two different cycles of tests have been made: the first after the application of the FRP vertical strips, and the second after inserting other FRP strips in the horizontal direction (double-reinforced panel, Fig. 5b).

In general it can be noticed that the major effect of the reinforcement application is the reduction of the stress in the masonry; lower displacements at the locations monitored by the transducers can be recorded with comparison to the unconsolidated case (Fig. 6a,b,c).

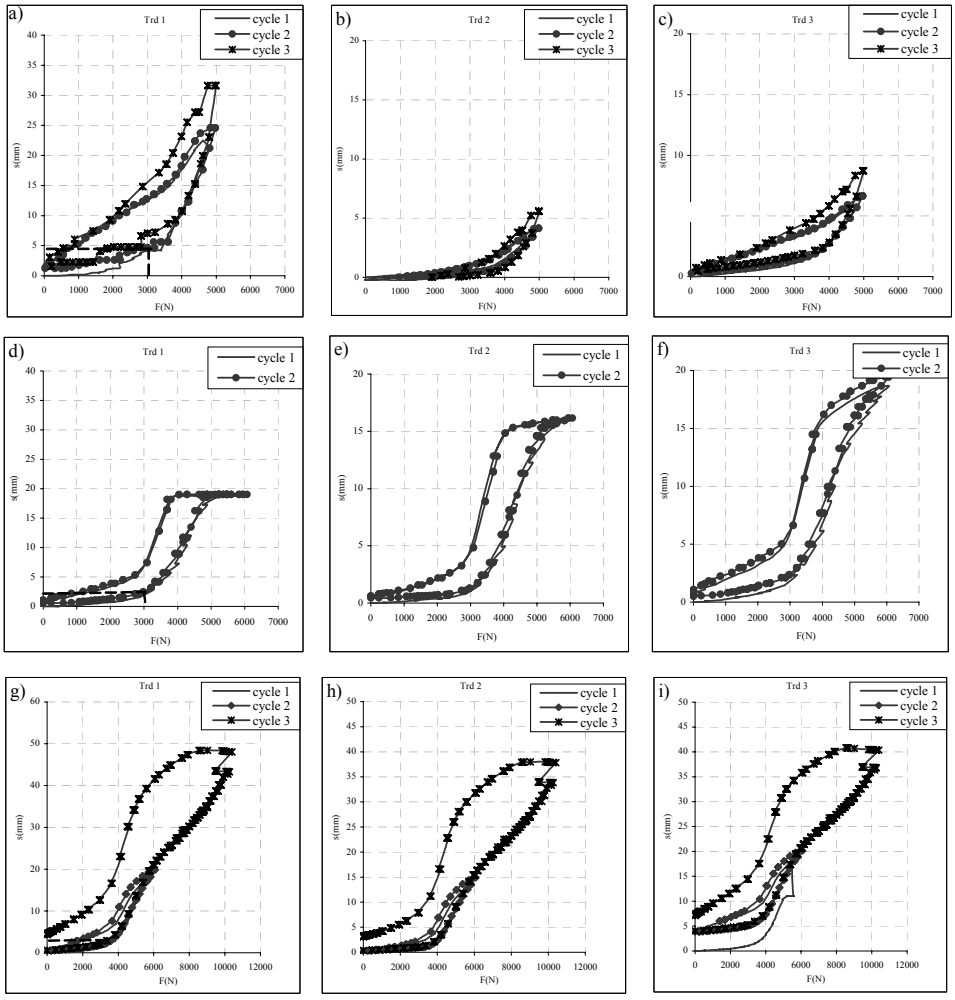

Figure 6 : Displacements recorded by the transducers 1, 2 and 3 on: (a)-(b)-(c) masonry panel, (d)-(e)-(f) FRP-reinforced panel, and (g)-(h)-(i) double-reinforced panel.

The increase of the overall stiffness of the panel results in a higher loading capacity with respect to the non-reinforced masonry wall (Fig. 6d,e,f). In details, with reference to the transducer 1 some considerations can be made. The trend of each curve shows that it is closer to the x-axis (representing the load variable), thus indicating an increase in the stiffness; it is also related to an higher collapse value of the load which by means of the reinforcements is going beyond a force value of 5000 N.

Moreover, for example, the displacements relevant to the force 3000 N are strongly reduced for the reinforced panel with respect to the not-reinforced one. The situation in terms of displacements and stiffness (Fig. 6g,h,i) becomes even more evident when other reinforcements are

superimposed such as some horizontal C-FRP strips disposed as shown in Fig. 5b). The collapse of the panel seems to be due, in this case, to a force higher than 6000 N.

6 CONCLUSIONS

In the paper an experimental survey concerned with the in-plane behaviour of some masonry walls is reported, intended to validate both the effectiveness of the NRT approach to yield computational models for the analysis of masonry panels with and without reinforcements, and the improvement of the structural pattern by FRP prostheses. Even light FRP additions prove to confer high improvement to the horizontal load-carrying capacity of the wall (as by a comparison of the results reported in Fig. 6). On the other side, the NRT model, which has been implemented in a computer code developed by the authors for research purposes, also proves to be able to catch very nearby the response of the wall both before and after the reinforcement, as demonstrated by some preliminary results (Baratta and Corbi 2001) and by research in progress and laboratory tests.

ACKNOWLEDGEMENTS

The present research has been performed thanks to the financial support by the Department of "Protezione Civile" of the Italian Government, through the RELUIS Pool (Convention n. 540 signed 07/11/2005, Research Line n. 8).

REFERENCES

Baratta, A. 1991. Statics and reliability of masonry structures, In F.Casciati & J.B.Roberts (Eds), *Reliability Problems: General Principles and Applications in Mechanics of Solids and Structures*, Udine: CISM.

Baratta, A. and Corbi, I. 2004. Iterative Procedure in No-Tension 2D Problems: theoretical solution and experimental applications. In G.C.Sih & L.Nobile (Eds.), "*Restoration, Recycling and Rejuvenation Technology for Engineering and Architecture Application*", p. 67-75, Bologna: Aracne Ed.

Baratta, A. and Corbi, I. 2003. Investigation of FRP consolidated masonry panels, *Proc. of the 9th Int. Conf. on Civil and Structural Engineering - CC03*, paper n. 99, The Netherlands.

Baratta, A. and Corbi, O. 2001. Metodi di Verifica delle Strutture Murarie Consolidate con l' Uso di Materiali Compositi, *Proc. 15th Nat. Congress of Theoretical and Applied Mechanic AIMETA'01*, Taormina, Italy (in Italian).

Baratta, A. and Corbi, O. 2005. On variational approaches in NRT continua, *J. of Solids and Structures*, 42, p. 5307-5321.

Baratta, A. and Toscano, R. 1982. Stati Tensionali in Pannelli di Materiale Non Reagente a Trazione, *Proc. 4th Nat. Congress of Theoretical and Applied Mechanic AIMETA*, Genova, Italy (in Italian).

Baratta, A. and Voiello, G. 1988. Teoria delle pareti in muratura a blocchi: un modello discretizzato di calcolo, In: *Franco Jossa e la sua opera*, Napoli: Giannini Ed..

Briccoli Bati, S. and Rovero, L. 2000. Consolidamento di Archi in Muratura con Nastri di Composito a Fibre Lunghe di Carbonio. *Proc. National Conference Mechanics of Masonry Structures Strengthened with FRP- Materials*, p. 53-64, Venice, Italy.

El-Badry, M. 1996. Advanced Composite Materials Bridges and Structures. *Proc. 2nd International Conference Advanced Composite Materials in Bridges and Structures*, Montréal.

Heyman, J. 1969. The safety of masonry arches, *Int. J. Mech. Sciences*, 11(2).

Rao, S.S. 1978. *Optimization: theory and applications*. Wiley (Ed), E.L., Meerut, India.

Schwegler, G. 1994. Masonry Construction Strengthened with Fiber Composites in Seismically Endangered Zones. *Proc. 10th European Conference of Earthquake Engineering*, Vienna.

Traintafillou, T.C. 1996. Innovative Strengthening of Masonry Monuments with Composites. *Proc. 2nd International Conference Advanced Composite Materials in Bridges and Structures*, Montréal.